IOP Publishing New J. Phys. 27 (2025) 054504 https://doi.org/10.1088/1367-2630/add367

New Journal of Physics
The open access journal at the forefront of physics

Deutsche Physikalische Gesellschaft DPG
IOP Institute of Physics

Published in partnership with: Deutsche Physikalische Gesellschaft and the Institute of Physics

OPEN ACCESS

RECEIVED
9 March 2025

REVISED
26 April 2025

ACCEPTED FOR PUBLICATION
2 May 2025

PUBLISHED
9 May 2025

PAPER

Long-range quantum correlations based on quantum coherence in a hybrid system

Guanghui Wang[1,2,*], **Xiao Wu**[2], **Dongyan Lü**[3], **Yuan Zhou**[4], **Zeyun Shi**[4], **Xinke Li**[3] and **Yaojia Chen**[5]

[1] Hubei Key Laboratory of Automotive Power Train and Electronic Control, Shiyan 442002, People's Republic of China
[2] School of Automotive Engineering, Hubei University of Automotive Technology, Shiyan 442002, People's Republic of China
[3] School of Science, Hubei University of Automotive Technology, Shiyan 442002, People's Republic of China
[4] School of Electrical and Information Engineering, Hubei University of Automotive Technology, Shiyan 442000, People's Republic of China
[5] School of Electronic Engineering, Wuhan Vocational College of Software and Engineering, Wuhan 430205, People's Republic of China
[*] Author to whom any correspondence should be addressed.

E-mail: ghwang2020@huat.edu.cn

Keywords: hybrid, quantum correlations, nitrogen-vacancy (NV) centers, Kerr nonlinearity, one-way Einstein–Podolsky–Rosen steering, spin squeezing

Abstract

We propose a scheme to realize long-range quantum correlations of two separated ensembles of nitrogen-vacancy (NV) centers via asymmetric driving. Either of the ensembles of NV centers is dynamically driven by a strong applied microwave field, which causes the coupled energy levels to split into dressed states. A quantum electromechanical system (QEMS), as a quantum data bus, connects the two ensembles of NV centers. When a weak microwave field in QEMS couples the same energy level transitions of the two ensembles of NV centers, the beam-splitter-like interactions are realized. The collective mode of the mechanical resonators in the QEMS is near-resonant with the dressed energy level establishing the parametric down-conversion-like interaction. The Kerr nonlinearity produced by the parametric down-conversion-like interaction can be transferred by the beam-splitter-like interactions. We demonstrate the photon-phonon one-way Einstein–Podolsky–Rosen steering, and spin squeezing. Our scheme can thereafter support a potential application of the generalized storage of quantum information.

1. Introduction

With the rapid advancement of quantum technology, hybrid quantum systems have emerged as one of the most reliable platforms for quantum simulation and manipulation [1–4]. Among these, solid-state spins such as nitrogen-vacancy (NV) centers and silicon-vacancy centers offer several advantages, including long coherence times, ease of control, and no need for trapping. These spins can also strongly interact with various quantum devices, such as optical cavities (including microwave and acoustic cavities), superconducting circuits (SC), and mechanical resonators (MRs). Therefore, a promising platform for quantum information processing (QIP) can be established [5–21]. Recently, research on mechanical and acoustic quantum manipulation has accelerated due to advances in cryogenic cooling technology [22–24]. To date, many different solid-state spins have been reported to be manipulatable by MR through gradient magnetic or strain fields, such as the strong coherent NV-MR coupling proposed in [25]. Long-range spin–spin interactions between separated NV centers can be realized through SC, MRs, and acoustic cavities [23, 26, 27]. Additionally, quantum interference of photons emitted from two remote NV centers has been observed [28–30].

Einstein–Podolsky–Rosen (EPR) steering represents a special form of entanglement that bridges quantum state inseparability and Bell non-locality [31, 32]. More interestingly, unlike traditional entanglement, EPR steering can exhibit a natural asymmetry [33] and potentially lead to non-reciprocal quantum entanglement, such as one-way EPR steering [34]. One-way EPR steering, enabled by inherent symmetry breaking, has been demonstrated both theoretically and experimentally in various quantum

systems [35–41]. It has found widespread applications in QIP, including quantum teleportation [42–44], quantum secret sharing [45–47], quantum key distribution [48–50], and quantum computing [51].

In this work, we study a hybrid quantum system consisting of two homogeneous NV ensembles interacting with a quantum electromechanical system (QEMS). Either of the ensemble of NV centers is dynamically driven by a strong applied microwave field, which causes the coupled energy levels to split into dressed states. The QEMS, as a quantum bus, connects the two ensembles of NV centers, separated by a distance of $d = 100\ \mu$m [26]. A microwave field in QEMS couples the same energy levels of the two ensembles of NV centers, realizing the beam-splitter-like interactions between them. The collective mode of the MRs in the QEMS is near-resonant with the dressed energy level establishing the parametric down-conversion-like interaction. Photon–phonon one-way EPR steering is realized through down-conversion-like and beam-splitter-like interactions in our system. Meanwhile, spin squeezing occurs in the ground states of the bare NV centers. Our scheme demonstrates the transfer of the nonlinear effect between two ensembles of NV centers using two resonators and a microwave field. Our scheme minimizes system dissipation to preserve coherence, contrasting with the approach that uses dissipation to establish quantum correlations in [30].

The remainder of this article is organized as follows, section 2 presents hybrid quantum system and Hamiltonian. Quantum-coherence-based nonlinearity of two separated ensembles of NV centers is demonstrated in section 3. Section 4 shows long-rang one-way EPR steering. Section 5 presents spin squeezing at the steady state. Experimental considerations and potential applications are shown in section 6. Finally, our conclusions are summarized in section 7.

2. Hybrid quantum system and Hamiltonian

As illustrated in figure 1, two separated ensembles of NV centers (NV_1 and NV_2) are connected by an EMQS. The triple ground states of the single NV center denote $|0\rangle$ and $|\pm1\rangle$. The zero-field splitting between the levels $|0\rangle^{(1)}$ and $|\pm1\rangle^{(1)}$ is $D_0 = 2\pi \times 2.87$ GHz, and the Zeeman splitting $\delta_B = 2g_e\mu_B B_{\text{static}}$ induced by a homogeneous static magnetic field B_{static} removes the degeneracy between the levels $|\pm1\rangle$, where $g_e \simeq 2$ is the Landé factor of NV center and $\mu_B = 14$ GHz/T is the Bohr magneton. We assume that the MR in the EQMS has dimensions of (l, w, t). The NV_1 centers are initially driven by a strong microwave field with Rabi frequency Ω. In the interaction picture, the Hamiltonian of the NV_1 centers is given by the unitary operator $U(t) = e^{-i\omega_1\sigma^{(1)}_{+1+1}t}$ [52, 53], is

$$H_{\text{NV}} = \Delta^{(1)}_{+1}\sigma^{(1)}_{+1+1} + \frac{\Omega}{2}\left(\sigma^{(1)}_{+10} + \sigma^{(1)}_{0+1}\right), \tag{1}$$

where $\Delta^{(1)}_{+1} = \omega^{(1)}_{+1} - \omega_1$ is the detuning between the transition frequency $\omega^{(1)}_{+1}$ and the driving frequency ω_1. $\sigma^{(1)}_{k,l} = \sum_{i=1}^{N}\sigma^{i(1)}_{kl}$ are the projection operators for $k = l$ and the spin-flip operators for $k \neq l$ [54, 55]. $\Omega = -\mu_{+10}\varepsilon$, μ_{+10} is the electric dipole moment and ε is the electric amplitude. N is the number of NV centers. It is easily seen that the Hamiltonian (1) can be diagonalized

$$H_{\text{NV}} = \sum_{j=\pm} d_j\sigma_j, \tag{2}$$

where $d_\pm = (\Delta \pm \Omega_0)/2$ are the eigenvalues, $\Omega_0 = \sqrt{\Delta^2 + \Omega^2}$, $\Delta^{(1)}_{+1} = \Delta$, $\sigma_\pm = |\pm\rangle\langle\pm|$, and the eigenvectors are

$$\begin{aligned} |+\rangle &= \sin\theta\,|0\rangle^{(1)} + \cos\theta\,|+1\rangle^{(1)}, \\ |-\rangle &= \cos\theta\,|0\rangle^{(1)} - \sin\theta\,|+1\rangle^{(1)}, \end{aligned} \tag{3}$$

where $\sin\theta = \sqrt{(\Omega_0 - \Delta)/2\Omega_0}$ and $\cos\theta = \sqrt{(\Omega_0 + \Delta)/2\Omega_0}$. For the ensemble of NV_1 centers, equations (3) are generally referred to as 'dressed states'.

Two identical charged cantilever MRs, with sharp magnetic tips attached to their free ends, couple magnetically to the two ensembles of NV centers. As in [26], the charged MRs capacitively interact with the electromechanical quantum bus, contributing to the coupling between the vibrational modes (frequency ν_r) and the NV centers. The vibrational modes of the two MRs are renormalized as

$$H_{\text{vm}} = \sum_{i=1,2}\nu_r b_i^\dagger b_i + \frac{g_{12}}{2}\left(b_1 + b_1^\dagger\right)\left(b_2 + b_2^\dagger\right) = \nu_R b^\dagger b + \nu_D b_D^\dagger b_D, \tag{4}$$

where b and b_D mean the mode operators of collective phonon eigenmodes of the two MRs, and ν_R and ν_D are the frequencies of the collective mode, respectively. Here, mode b satisfies the resonant or near-resonant

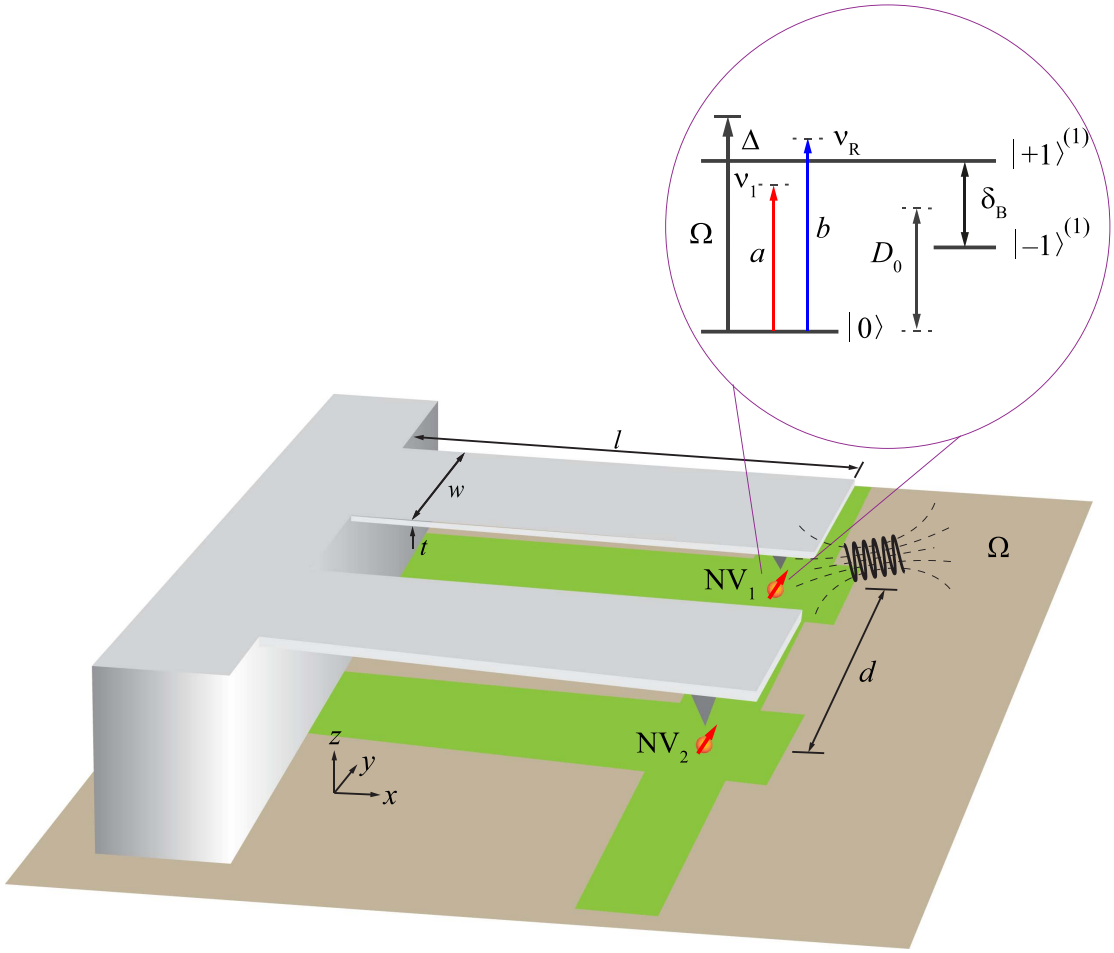

Figure 1. Schematic illustration of long-range quantum correlations. Two separated ensembles of NV centers (NV_1 and NV_2 with a distance of $d \simeq 100\ \mu$m) are connected by an EMQS. A strong applied microwave field with Rabi frequency Ω dynamically drives NV_1 to split the energy levels (dressed energy levels). A weak microwave field and two identical MRs in the QEMS simultaneously couple the dressed energy levels of NV_1 centers and the bared energy levels of NV_1 centers. The inset shows the energy levels of the triplet ground states of the NV_1 center. Here, $D_0 = 2\pi \times 2.87$ GHz is the zero-field splitting, and $\delta_B = 2g_e\mu_B B_{\text{static}}$ is the Zeeman splitting. The weak microwave field a and the collective mode b of the mechanical resonators with the circular frequencies ν_1 and ν_R respectively couple these two level. The NV_2 center has the same level structure as the NV_1 centers.

condition, while b_D represents a far off-resonant mode. We can safely discard b_D in the subsequent analysis. When the collective mode b couples the transition from $|0\rangle$ to $|+1\rangle$, the Hamiltonian is given by

$$H_{\text{NR}} = \nu_R b^\dagger b + \sum_{j=1,2} G_j \left(b\sigma_{+10}^{(j)} + b^\dagger \sigma_{0+1}^{(j)} \right), \tag{5}$$

where $G_j = g_e\mu_B\chi_j a_0$ $(j = 1, 2)$, χ_j are the magnetic field gradients, and $a_0 = 1/\sqrt{2m\nu_R}$. In the rotating frame of $H_R = \delta_2 b^\dagger b + d_+\sigma_{++} + d_-\sigma_{--} + \omega_2\sigma_{+1+1}^{(2)}$ and the rotating wave approximation, Hamiltonian (5) can be rewritten as follows (see appendix A)

$$H_{\text{NR}} = \delta_R b^\dagger b + \lambda \left(b\sigma_{-+} + b^\dagger \sigma_{+-} \right), \tag{6}$$

where $\delta_R = \nu_R - \delta_2$, $\lambda = -G_1 \sin\theta\cos\theta$, $\delta_2 = -\Omega_0$, δ_2 and ω_2 are the driving frequencies of the vibrational modes and NV_2. In this Hamiltonian, the term $b\sigma_{-+}$ denotes a nonlinear process in which the dressed-state transition from $|+\rangle$ to $|-\rangle$ accompanies with the absorption of a phonon. The terms $b\sigma_{-+}$ and $b^\dagger\sigma_{+-}$ are referred to as the parametric down-conversion interactions.

A weak microwave field in the QEMS with the circular frequency ν_1 couples the two ensembles of NV centers, the Hamiltonian is written as follows (see appendix B) [16, 56, 57]

$$H_{\text{NC}} = (\Lambda a\sigma_{+-} + g_2 a\sigma_{+10}) + \text{H.c.} + \delta_c a^\dagger a, \tag{7}$$

where $\delta_c = \nu_1 - \delta_1$, and δ_1 are the driving frequencies of the microwave field. $\Lambda = g_1\cos^2\theta$, H.c. means the Hermite conjugation. $a(a^\dagger)$ is the annihilation(creation) operator of the microwave field, and the coupling

strength g_j $(j=1,2)$ of the NV centers and microwave field can be enhanced by the factor of $\sqrt{N}$. In what follows, we just consider the dressed states $|\pm\rangle$ for NV_1 centers and the naked states $\sigma_{kl}^{(2)}$ $(k,l=0,\pm1)$ for NV_2 centers. Therefore, the superscript number '(2)' of $\sigma_{kl}^{(2)}$ can be omitted for simplicity. In the Hamiltonian (7), the term $a\sigma_{+-}$($a\sigma_{+10}$) signifies that the transition from $|-\rangle(|0\rangle)$ to $|+\rangle(|+1\rangle)$ accompanies with the absorption of a phonon, which is termed a beam-splitter-like interaction. Now the cooperative parameters can be introduced $C_{1,2}=g_{1,2}^2/\kappa_{1,2}\gamma_{1,2}$ and $C_3=G_1^2/\kappa_2\gamma_1$.

The total Hamiltonian of the hybrid system under consideration reads

$$H=H_{\rm NV}+H_{\rm NR}+H_{\rm NC}. \tag{8}$$

The master equation takes the form [58]

$$\dot{\rho}=-i[H,\rho]+\sum_{j,l=1,2,}\frac{\gamma_l}{2}\mathcal{L}_{\sigma_{0+1}^{(j)}}+\sum_{j,l=1,2,}\frac{\kappa_l}{2}\mathcal{L}_{a,b}, \tag{9}$$

where the damping term $\mathcal{L}\rho=2o\rho o^\dagger-o^\dagger o\rho-\rho o^\dagger o$, γ_l are the decay rates of the NV centers, $\kappa_{1,2}$ are the decay rates of the microwave fields and MRs. From an experimental perspective, our scheme achieves ideal fidelities under conditions similar to those reported in [26], where the mechanical quality factor is approximately $Q_{\rm m}\sim10^6$ at $T=100$ mK [26].

3. Quantum-coherence-based nonlinearity of two separated ensembles of NV centers

Generally, the interaction between the optical field and matter can be expressed using the Dicke model, which has the form $H\sim(a+a^\dagger)(b+b^\dagger)$. The terms ab and $a^\dagger b^\dagger$, similar to the parameter down-conversion process, produce nonlinear interactions indicative of a parametric down-conversion-like interaction. Alternatively, the terms $ab^\dagger$ and $ba^\dagger$ induce linear interactions through photon hopping, which play a role in beam splitters and are termed beam-splitter-like interactions. Related to quantum correlations is one-way EPR steering which is intermediate between entanglement and Bell nonlocality [59]. Many schemes based on Kerr nonlinearity in various quantum systems have been proposed to realize quantum steering [60–63]. Electromagnetically induced transparency (EIT) is one of the representative schemes for Kerr nonlinearity [64, 65]. Especially, enhanced Kerr nonlinearity has been demonstrated in theory and experiment [66, 67]. Recently, the electromagnetically-induced-transparency-like (EIT-like) phenomenon has been shown in two separated ensembles of atoms in an optical cavity [68, 69]. The physical essence is quantum coherence produced by two separate ensembles of two-level atoms interacting with the applied optical fields.

From Hamiltonian (8), NV_2 centers just interact with microwave field a and play a role of the beam splitter, which produces linear interaction and establishes the quantum correlations of the two separated ensembles of NV centers. However, NV_1 centers simultaneously interact with microwave field a and collective mode b of the MRs. Consequently, down-conversion-like and beam-splitter-like interactions occur at the same time. As illustrated in figure 2, the dressed transitions $|+\rangle\overset{a^\dagger,b}{\underset{a,b^\dagger}{\rightleftharpoons}}|-\rangle$ of NV_1 centers establish the parametric down-conversion-like and beam-splitter-like interactions in this process. The transitions $|+1\rangle\overset{a^\dagger}{\underset{a}{\rightleftharpoons}}|0\rangle$ of $NV_{1,2}$ centers lead to beam-splitter-like interactions between the both ensembles of NV centers and microwave field. The long-range quantum correlations between the separated NV_1 and NV_2 centers are established by the beam-splitter-like interactions $NV_1\overset{a}{\underset{a^\dagger}{\longleftrightarrow}}NV_2\overset{a}{\underset{a^\dagger}{\longleftrightarrow}}NV_1$, as shown in figure 3.

This beam-splitter-like interactions ($a\sigma_{+-}$, $a\sigma_{+10}$, $a^\dagger\sigma_{-+}$ and $a^\dagger\sigma_{01+}$) play central role in the realization of long-range EPR steering, which makes the nonlinear transfer between the subsystems.

In general, the response of NV_1 centers to the microwave field and collective mode of the MRs can be described by the susceptibility $\chi=-\mu_{-+}\rho_{+-}/\epsilon_0\varepsilon$ (ϵ_0 is the permittivity of free space). It is well known that the real part Reχ of the susceptibility relates to dispersion. Plotted in figure 4 is that the dispersion Reχ in unit of $|\mu_{-+}|^2/\epsilon_0$ versus the normalized detuning Δ/Ω with the parameters $\delta_{\rm R}=\delta_c=0$, $C_1=50\gamma$, $\kappa_1=10\kappa_2=\gamma$, $\gamma_2=100\gamma_1=\gamma$, $\omega=0$, $C_{2,3}=50\gamma$ (black circle), $C_{2,3}=100\gamma$ (red circle), $C_{2,3}=200\gamma$ (blue circle), and $\omega=0.1\gamma$, $C_{2,3}=200\gamma$ (magenta square), respectively. It is obvious that the dispersive profiles are similar to that of EIT, which further verifies quantum correlation can be generated in the long-range two-level subsystems [58].

Before proceeding further, the master equations (9) can be transformed into sets of c-number Langevin equations under the generalized P representation [70]. The correspondences between the c-number variables

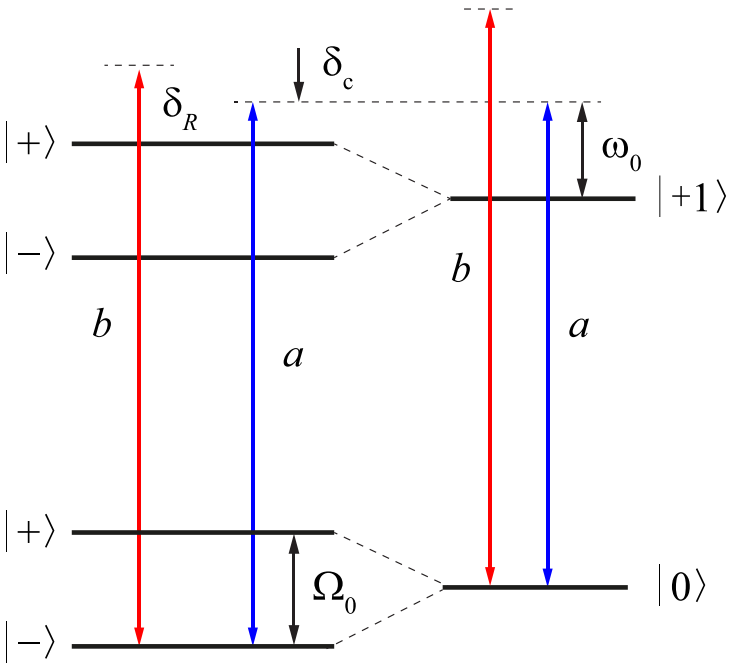

Figure 2. Schematic of the photon-spin-phonon interactions. Left: The dressed levels $|\pm\rangle$ of NV_1 centers interact with the microwave field a and the collective mode b of the mechanical resonators at the same time, which produces beam-splitter-like interaction ($a\sigma_{+-}$ in equation (7)) and parametric down-conversion-like interaction ($b\sigma_{-+}$ in equation (6)). Right: The naked levels $|+1,0\rangle$ of NV_2 centers interact with microwave field a, in which only the beam-splitter-like interaction ($a\sigma_{+10}$ in equation (7)) occurs. In this process, the long-range separate NV centers are connected by the microwave field a based on the the beam-splitter-like interactions ($a\sigma_{+-}$, and $a\sigma_{+10}$ in equation (7)). The mode b is far-off resonant with its coupled transition.

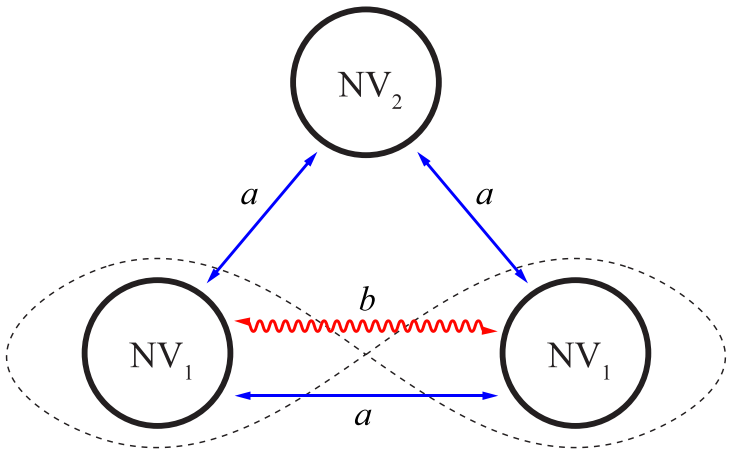

Figure 3. Schematic of the interactions between the NV centers, microwave field and EMQB. NV_2 centers just interact with the microwave field (see equation (6)), in which only the beam-splitter-like interaction is produced. The collective mode of the mechanical resonators interacting with NV_1 centers only leads to the parametric down-conversion-like interaction.

and operators are shown in the appendix C. The Langevin equations read as follows

$$\begin{aligned}
\dot{\alpha} &= -\left(\frac{\kappa_1}{2} + i\delta_c\right)\alpha + \Lambda\nu_1 + g_2\nu_2 + \sqrt{\kappa_1}\alpha_{\text{in}},\\
\dot{\beta}^* &= -\left(\frac{\kappa_2}{2} - i\delta_{\text{R}}\right)\beta^* - \lambda\nu_2 + \sqrt{\kappa_2}\beta^*_{\text{in}},\\
\dot{\nu}_1 &= -\frac{\Gamma}{2}\nu_1 + \pi_1\left(\Lambda\alpha + \lambda\beta^*\right) + F_{\nu_1},\\
\dot{\nu}_2 &= -\frac{\gamma_2}{2}\nu_2 + \pi_2 g_2\alpha + F_{\nu_2},
\end{aligned} \tag{10}$$

where the conjugations and closed relations $\langle\sigma_{++}\rangle + \langle\sigma_{--}\rangle = \langle\sigma_{ee}\rangle + \langle\sigma_{gg}\rangle = N$ are considered. $\Gamma = 4\Gamma_1 + \Gamma_2 + \Gamma_3$, $\pi_1 = \langle\sigma_{++}\rangle - \langle\sigma_{--}\rangle$, $\pi_2 = \langle\sigma_{+1+1}\rangle - \langle\sigma_{00}\rangle$. $\langle\cdot\rangle$ denotes the mean value. α_{in}, β_{in} and F_{ν_l}

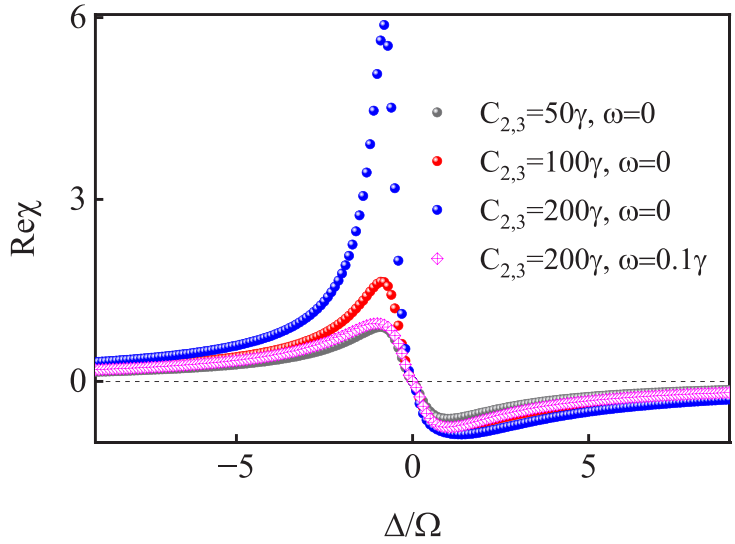

Figure 4. Schematic of the nonlinearities of NV_1 centers response to the microwave field and collective mode. Reχ in unit of $|\mu_{-+}|^2/\epsilon_0$ versus the normalized detuning Δ/Ω with the parameters $\delta_R = \delta_c = 0$, $C_1 = 50\gamma$, $\kappa_1 = 10\kappa_2 = \gamma$, $\gamma_2 = 100\gamma_1 = \gamma$, $\omega = 0$, $C_{2,3} = 50\gamma$ (black circle), $C_{2,3} = 100\gamma$ (red circle), $C_{2,3} = 200\gamma$ (blue circle), and $\omega = 0.1\gamma$, $C_{2,3} = 200\gamma$ (magenta square), respectively.

$(l = 1, 2)$ are noise terms with zero means. In the Fourier domain, the solutions of equations (10) are obtained

$$\begin{aligned}
\alpha &= \frac{t\sqrt{\kappa_1}\alpha_{in} + r\sqrt{\kappa_2}\beta_{in}^*}{st + r^2}, \\
\beta^* &= \frac{s\sqrt{\kappa_2}\beta_{in}^* - r\sqrt{\kappa_1}\alpha_{in}}{st + r^2}, \\
\nu_1 &= \frac{\pi_1\Lambda}{\frac{\Gamma}{2} - i\omega}\alpha + \frac{\pi_1\lambda}{\frac{\Gamma}{2} - i\omega}\beta^*, \\
\nu_2 &= \frac{\pi_2 g_2}{\frac{\gamma_2}{2} - i\omega}\alpha,
\end{aligned} \tag{11}$$

where the coefficients read

$$\begin{aligned}
s &= \frac{\kappa_1}{2} + i(\delta_c - \omega) - \frac{\pi_1\Lambda^2}{\frac{\Gamma}{2} - i\omega} - \frac{\pi_2 g_2^2}{\frac{\gamma_2}{2} - i\omega}, \\
t &= \frac{\kappa_2}{2} - i(\delta_R - \omega) + \frac{\pi_1\lambda^2}{\frac{\Gamma}{2} - i\omega}, \\
r &= \frac{\pi_1\Lambda\lambda}{\frac{\Gamma}{2} - i\omega}.
\end{aligned}$$

4. Long-rang one-way EPR steering

In order to show one-way EPR steering, the amplitude and phase quadratures are defined $X_j = o + o^\dagger$ and $Y_j = -i(o - o^\dagger)$ $(o = a, b)$. Fortunately, the sufficient and necessary criterion for detection of the steering of Gaussian states under the Gaussian measurements is presented by Reid [43]. For microwave field a and collective mode b, the criteria of the steering from a to b and b to a are [71–73]

$$V_{2\leftarrow 1} = V_{inf}(X_2)\, V_{inf}(Y_2) < 1, \tag{12}$$

$$V_{1\leftarrow 2} = V_{inf}(X_1)\, V_{inf}(Y_1) < 1, \tag{13}$$

where $V_{inf}(o_k) = V(o_k) - \langle o_k o_l\rangle^2 / V(o_l)$, $V(o_k) = \langle(\delta o_k)^2\rangle - \langle \delta o_k\rangle^2$, and $o_k = X_k, Y_k$ $(k \neq l = 1, 2)$. As only one of the criteria (12) and (13) holds, the one-way EPR steering occurs. Meanwhile, we suppose that initial state of Alice and Bob is $|\psi\rangle = |\varphi\rangle_A \otimes |\varphi\rangle_B$. Alice and Bob operate their states by microwave field a and collective mode b, respectively.

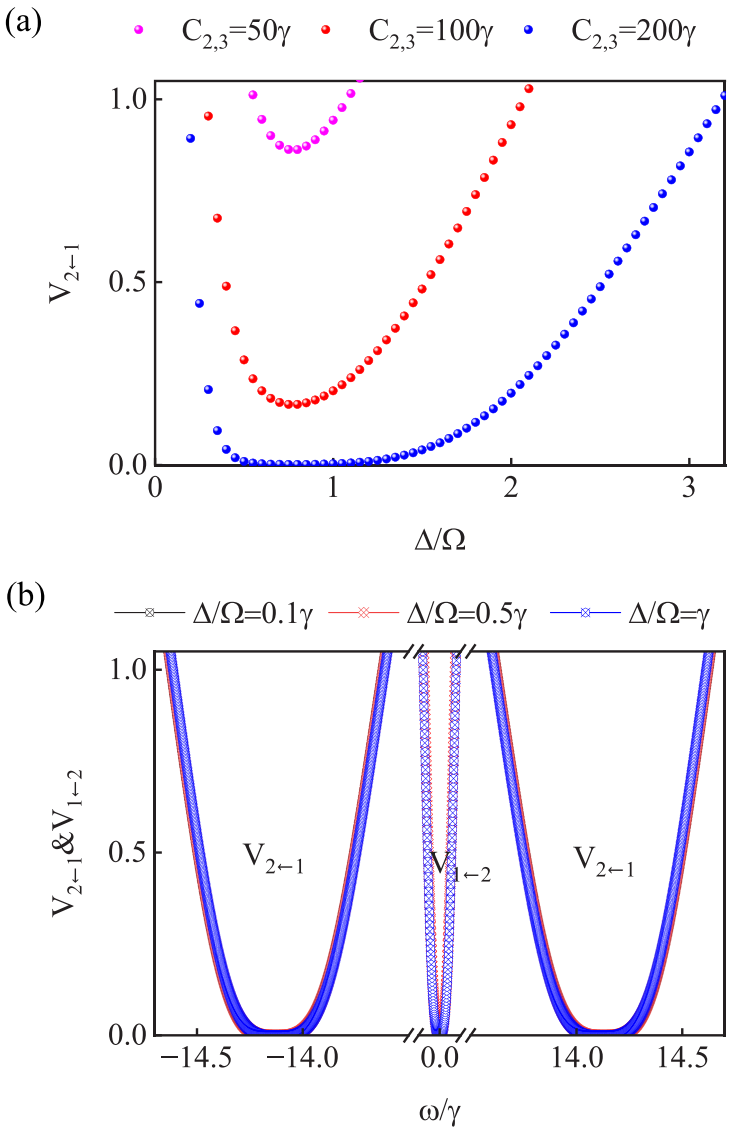

Figure 5. Schematic of criteria $V_{2\leftarrow1}$ and $V_{1\leftarrow2}$. (a) Criterion $V_{2\leftarrow1}$ versus the normalized detuning Δ/Ω with the parameters $\delta_R = \delta_c = 0$, $\kappa_1 = 10\kappa_2 = \gamma$, $\gamma_2 = 100\gamma_1 = \gamma$, $C_1 = 50\gamma$, and $C_{2,3} = 50\gamma$, 100γ, 200γ, respectively. $V_{1\leftarrow2}$ are always more than unit. (b) Criteria $V_{2\leftarrow1}$ and $V_{1\leftarrow2}$ versus the normalized frequency ω/γ with the parameters $\delta_R = \delta_c = 0$, $\kappa_1 = 10\kappa_2 = \gamma$, $\gamma_2 = 100\gamma_1 = \gamma$, $C_1 = 50\gamma$, $C_{2,3} = 200\gamma$, and $\Delta/\Omega = 0.1\gamma$, 0.5γ, and γ.

Consider the input–output relations $o^{\text{out}} + o^{\text{in}} = \sqrt{k_j}o$ ($j = 1, 2$ and $o = \alpha, \beta$). According to equations (11), the criterions read as follows

$$V_{2\leftarrow1} = 4\left[|M|^2 + |Q|^2 - \frac{\text{Re}\,(MP^* - MQ)^2}{2\left(|M|^2 + |P|^2\right)}\right]^2, \tag{14}$$

$$V_{1\leftarrow2} = 4\left[|M|^2 + |P|^2 - \frac{\text{Re}\,(MP^* - MQ)^2}{2\left(|M|^2 + |Q|^2\right)}\right]^2, \tag{15}$$

where $M = r\sqrt{\kappa_1\kappa_2}/(st + r^2)$, $P = t\kappa_1/(st + r^2) - 1$, $Q^* = s\kappa_2/(st + r^2) - 1$.

Plotted in figure 5 are the criteria $V_{2\leftarrow1}$ and $V_{1\leftarrow2}$. At the steady state, $V_{1\leftarrow2}$ are always more than unit. The criterion $V_{2\leftarrow1}$ versus the normalized detuning Δ/Ω with the parameters $\delta_R = \delta_c = 0$, $\kappa_1 = 10\kappa_2 = \gamma$, $\gamma_2 = 100\gamma_1 = \gamma$, $C_1 = 50\gamma$, and $C_{2,3} = 50\gamma$, 100γ, 200γ, as illustrated in figure 5(a). The criteria $V_{2\leftarrow1}$ and $V_{1\leftarrow2}$ versus the normalized frequency ω/γ with the parameters $\delta_R = \delta_c = 0$, $\kappa_1 = 10\kappa_2 = \gamma$, $\gamma_2 = 100\gamma_1 = \gamma$, $C_1 = 50\gamma$, $C_{2,3} = 200\gamma$, and $\Delta/\Omega = 0.1\gamma$, 0.5γ, and γ, as shown in figure 5(b). It is easily seen that microwave field a can steer collective mode b of the MRs ($V_{2\leftarrow1} < 1$) at the steady state. In this case, it means that Alice can operate the initial state $|\psi\rangle$ by microwave field a, but Bob cannot do anything. This

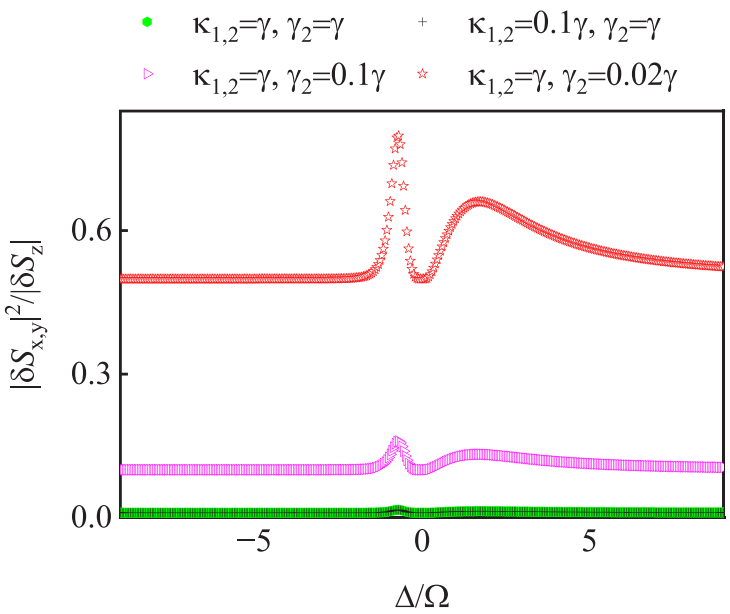

Figure 6. $|\delta S_{x,y}|^2 / |\delta S_z|$ versus the normalized detuning Δ/Ω with the parameters $\delta_R = \delta_c = 0$, $C_1 = 50\gamma$, $C_{2,3} = 200\gamma$, $\gamma_1 = 0.01\gamma$, $\kappa_{1,2} = 0.1\gamma$, $\gamma_2 = \gamma$, and $\kappa_{1,2} = \gamma$, $\gamma_2 = \gamma, 0.1\gamma, 0.02\gamma$, respectively.

asymmetrical operations for the quantum states are referred as to one-way EPR steering which has been used widely for quantum secret sharing [45–47] and quantum key distribution [48–50]. In addition, one-way EPR steering from b to a ($V_{1\leftarrow 2} < 1$) and a to b ($V_{2\leftarrow 1} < 1$) can also occur in different frequency domain.

5. Spin squeezing at the steady state

As mentioned above, the system nonlinearities arise from the parametric down-conversion-like interactions between NV_1 centers and the collective mode of the MRs. However, NV_2 centers interacting with microwave field just produces beam-splitter-like interactions. Therefore, of interest for us is the nonlinearity of NV_2 centers. Now we check the spin components of NV_2 centers. At the steady state, $\langle S_x \rangle = \langle S_y \rangle = 0$ and $\langle S_z \rangle = -\pi_2$. Therefore, the spin squeezing is governed by the inequalities as follows [74, 75]

$$\left\langle \delta S_{x,y}^2 \right\rangle < |\langle \delta S_z \rangle| . \tag{16}$$

Form equations (11), the variances of the ground-state spin can be obtained

$$\frac{|\delta S_{x,y}|^2}{|\delta S_z|} = \frac{8|\pi_2||g_2|^2}{\gamma_2} \left(\left| \frac{t\sqrt{\kappa_1}}{st + r^2} \right|^2 + \left| \frac{r\sqrt{\kappa_2}}{st + r^2} \right|^2 \right), \tag{17}$$

and

$$\frac{|\delta S_{x,y}|^2}{|\delta S_z|} = \frac{8|\pi_2||g_2|^2}{\gamma_2} \left(\left| \frac{t'\sqrt{\kappa_1}}{s't' - r'^2} \right|^2 + \left| \frac{r'\sqrt{\kappa_2}}{s't' - r'^2} \right|^2 \right). \tag{18}$$

As illustrated in figure 6, $|\delta S_{x,y}|^2 / |\delta S_z|$ versus the normalized detuning Δ/Ω with the parameters $\delta_R = \delta_c = 0$, $C_1 = 50\gamma$, $C_{2,3} = 200\gamma$, $\gamma_1 = 0.01\gamma$, $\kappa_{1,2} = 0.1\gamma$, $\gamma_2 = \gamma$, and $\kappa_{1,2} = \gamma$, $\gamma_2 = \gamma, 0.1\gamma, 0.02\gamma$, respectively. It is obvious that the spin squeezing occurs in NV_2 centers. Such nonlinearities can transfer from NV_1 to NV_2 centers based on the beam-splitter-like interactions $NV_1 \overset{a}{\longleftrightarrow} NV_2 \overset{a}{\longleftrightarrow} NV_1$ as shown in figure 3. The quantum correlations of two ensembles of NV centers are established. It means that the quantum information can be stored in NV_2 centers based on the beam-splitter-like interactions.

6. Experimental considerations and potential applications

To examine the feasibility of our scheme for experiment, the silicon MR with dimensions ($l = 2$, $w = 0.1$, $t = 0.1$) μm is considered. The resonance frequency $\omega_r/2\pi \sim 1$ GHz and coupling strength $g/2\pi \sim 3$ kHz

with Young's modulus $E \sim 1.3 \times 10^{11}$ Pa and the mass density $\rho \sim 2.33 \times 10^3$ kg m^{-3}. The quality factor Q of the MR is about 10^6, $\gamma_m = \omega_r/Q$. As mentioned above, $g_c \propto \sqrt{N}$ which can match the coupling strength g_m. The pump fields frequencies are $\omega_+ \sim 3.3$ GHz, $\omega_2 \sim 2.3$ GHz, and the amplitudes are $\Omega_\pm \sim 1$ MHz [76]. Although the physical mechanics differ from those in [30], the feasible experimental conditions described therein inspire the realization of our scheme.

For applications, acoustic quantum devices are believed to have some unique advantages to accomplish potential targets of QIP, i.e. easy isolation environmental phononic noise than traditional electromagnetic systems, convenient fabrication because of their inherent large dimensions, rich hybridization choices to different quantum units with the strong coherent couplings but without any trap design. Therefore, utilizing the mechanical cantilever to engineer solid-state spins into the one-way EPR steering entanglement and spin squeezing corresponds to the feature of our scheme. Furthermore, we also state that such entanglement can potentially provide some interesting applications, such as the one-sided device-independent quantum communication [49, 50, 77], preparation, manipulation and measurement of the entanglement [78–82], quantum simulation [83, 84] *et al.*

7. Conclusion

In our scheme, two ensembles of the separated $NV_{1,2}$ centers with a distance of about 100 μm connected by the QEMS. NV_1 centers are dynamically driven by the strong microwave field with Rabi frequency Ω to dress the coupled energy levels. When a microwave field couples the same energy level transitions of the two ensembles of NV centers, the beam-splitter-like interactions are realized. The collective mode of the MRs in the QEMS is near-resonant with the dressed energy level establishing the parametric down-conversion-like interaction. The Kerr nonlinearity produced by the parametric down-conversion-like interaction can be transferred by the beam-splitter-like interactions. We demonstrate the photon-phonon one-way EPR steering, and spin squeezing.

Data availability statement

All data that support the findings of this study are included within the article (and any supplementary files).

Acknowledgment

This work is supported by National Natural Science Foundation of China under Grant No. 12304357, Natural Science Foundation of Hubei Province under Grant Nos. 2022CFB457, 2023AFB891 and 2023AFB352, Program for Science and Technology Innovation Team in Colleges of Hubei Province Grant No. T2023012, Research Program of the Education Department of Hubei province Grant No. B2022395, open fund of Hubei Key Laboratory of Automotive Power Train and Electronic Control (Hubei University of Automotive Technology) under Grant Nos. ZDK1202102, ZDK12023B04, Doctoral Scientific Research Foundation of HUAT under Grant Nos. BK202008, and Chunhui Project Foundation of Education Department of China under Grant No. HZKY20220337, Outstanding Young Fund of HUAT No. 2023YQ01.

Appendix A. The interaction between the NV centers and the collective mode of the MRs

The interaction between the NV centers and the collective mode of the MRs is described by equation (5). Because of the asymmetric driving, the energy levels of NV_1 centers is dressed. Hamiltonian (5) is rewritten

$$\begin{aligned} H_{NR} = \nu_R b^\dagger b + b\{G_1[\sin\theta\cos\theta(\sigma_{++} - \sigma_{--}) \\ + \cos^2\theta\sigma_{+-} - \sin^2\theta\sigma_{-+}] + G_2\sigma_{+10}^{(2)}\} + \text{H.c.}. \end{aligned} \tag{A1}$$

When the collective mode b is near-resonant with the dressed-state transition from $|-\rangle$ to $|+\rangle$, we obtain Hamiltonian (6) under the rotating-wave approximation.

Appendix B. Effective Hamiltonian

A weak microwave field couples the two ensembles of NV centers at the same time, the Hamiltonian reads

$$H_{NC} = \nu_1 a^\dagger a + \sum_{j=1,2} g_j \left(a\sigma_{+10}^{(j)} + a^\dagger \sigma_{0+1}^{(j)}\right). \tag{B1}$$

In the dressed picture, the Hamiltonian (B1) can be rewritten as follows, according to equation (3)

$$\begin{aligned} H_{\mathrm{NC}} = & \nu_1 a^\dagger a + g_1 \sin\theta\cos\theta\left(a + a^\dagger\right)\left(\sigma_{++} - \sigma_{--}\right) \\ & + g_1\left(a\cos^2\theta - a^\dagger\sin^2\theta\right)\sigma_{+-} + g_1\left(a^\dagger\cos^2\theta - a\sin^2\theta\right)\sigma_{-+} \\ & + g_2\left(a\sigma_{+10}^{(2)} + a^\dagger\sigma_{0+1}^{(2)}\right). \end{aligned} \tag{B2}$$

In the rotating frame of $H_{\mathrm{R}} = \delta_2 b^\dagger b + d_+\sigma_{++} + d_-\sigma_{--} + \omega_2\sigma_{+1+1}^{(2)}$ and the rotating-wave approximation, we can obtain Hamiltonian (7) when $\delta_1 = \Omega_0 = \omega_2$.

Appendix C. Mater equation in the dressed picture

According to the equation (9), the damping term of NV_1 centers in the dressed picture reads

$$\begin{aligned} \mathcal{L}_{\sigma_{0+1}^1}\rho = & \frac{\Gamma_1}{2}\left(2\sigma_{++}\rho\sigma_{++} - \rho\sigma_{++}\sigma_{++} - \sigma_{++}\sigma_{++}\rho\right) \\ & + \frac{\Gamma_1}{2}\left(2\sigma_{--}\rho\sigma_{--} - \rho\sigma_{--}\sigma_{--} - \sigma_{--}\sigma_{--}\rho\right) \\ & + \frac{\Gamma_2}{2}\left(2\sigma_{+-}\rho\sigma_{-+} - \rho\sigma_{-+}\sigma_{+-} - \sigma_{-+}\sigma_{+-}\rho\right) \\ & + \frac{\Gamma_3}{2}\left(2\sigma_{-+}\rho\sigma_{+-} - \rho\sigma_{+-}\sigma_{-+} - \sigma_{+-}\sigma_{-+}\rho\right) \\ & - \Gamma_1\left(2\sigma_{++}\rho\sigma_{--} + \sigma_{--}\rho\sigma_{++}\right) \end{aligned} \tag{C1}$$

where $\Gamma_1 = \gamma_1\sin^2\theta\cos^2\theta$, $\Gamma_2 = \gamma_1\sin^4\theta$, and $\Gamma_3 = \gamma_1\cos^4\theta$.

The populations of $\mathrm{NV}_{1,2}$ centers at the steady state are obtained

$$\begin{aligned} \langle\sigma_{++}\rangle &= \frac{N\sin^4\theta}{\sin^4\theta + \cos^4\theta}, \\ \langle\sigma_{00}^2\rangle &= N. \end{aligned} \tag{C2}$$

Appendix D. The correspondences between the *c*-number variables and the operators

The correspondences between the c-number variables and the operators are written in order as follows

$$\begin{pmatrix} a & b & \sigma_{-+} & \sigma_{0+1} \\ \alpha & \beta & \nu_1 & \nu_2 \end{pmatrix}. \tag{D1}$$

Appendix E. The stability conditions of the hybrid system

The Routh–Hurwitz criterion [85–87] is under consideration for the stability of this hybrid system. According to equation (10), the stability conditions read respectively as follows

$$\begin{aligned} & A_1 > 0, \\ & A_3 > 0, \\ & A_4 > 0, \\ & A_1 * A_2 * A_3 > A_3^2 + A_1^2 * A_4, \end{aligned} \tag{E1}$$

where

$$\begin{aligned} A_1 &= \frac{1}{2}\left(\Gamma + \gamma_2 + \kappa_1 + \kappa_2\right), \\ A_2 &= \frac{1}{4}\left[\left(\Gamma + \gamma_2\right)\left(\kappa_1 + \kappa_2\right) + \left(\Gamma\gamma_2 + \kappa_1\kappa_2\right)\right] \\ &\quad + \pi_1\left(\lambda^2 - \Lambda^2\right) - \pi_2 g_2, \\ A_3 &= \frac{\pi_1\lambda^2}{2}\left(\gamma_2 + \kappa_1\right) - \frac{\pi_1\Lambda^2}{2}\left(\gamma_2 + \kappa_2\right) + \frac{\Gamma\gamma_2}{8}\left(\kappa_1 + \kappa_2\right) \\ &\quad + \frac{1}{8}\left(\kappa_1\kappa_2 - 4\pi_2 g_2^2\right)\left(\Gamma + \gamma_2\right), \end{aligned}$$

$$A_4 = \frac{\pi_1\gamma_2}{4}\left(\kappa_1\lambda^2 - \kappa_2\Lambda^2\right) - \frac{\pi_1\Gamma g_2^2\gamma_2}{4} - \pi_1\pi_2\lambda^2 g_2^2 + \frac{\Gamma\gamma_2\kappa_1\kappa_2}{16}, \tag{E2}$$

and the detunings $\delta_R = \delta_c = 0$.

ORCID iDs

Guanghui Wang https://orcid.org/0000-0001-7822-7027
Yuan Zhou https://orcid.org/0000-0003-3356-1800
Zeyun Shi https://orcid.org/0000-0003-4266-0691
Xinke Li https://orcid.org/0000-0001-6533-9388

References

[1] He Q Y and Reid M D 2013 Einstein-podolsky-rosen paradox and quantum steering in pulsed optomechanics *Phys. Rev. A* **88** 052121
[2] Kiesewetter S, He Q Y, Drummond P D and Reid M D 2014 Scalable quantum simulation of pulsed entanglement and einstein-podolsky-rosen steering in optomechanics *Phys. Rev. A* **90** 043805
[3] Tan H, Zhang X and Li G 2015 Steady-state one-way einstein-podolsky-rosen steering in optomechanical interfaces *Phys. Rev. A* **91** 032121
[4] Schnabel R 2015 Einstein-podolsky-rosen–entangled motion of two massive objects *Phys. Rev. A* **92** 012126
[5] Ripoll J J G 2022 *Quantum Information and Quantum Optics With Superconducting Circuits* (Cambridge University Press)
[6] Prawer S and Aharonovich I 2014 *Quantum Information Processing With Diamond: Principles and Applications* (Elsevier)
[7] Zhang M, Long Y, Zhao S and Zhang X 2022 Einstein-podolsky-rosen steering and monogamy relations in controllable dynamical casimir arrays *Phys. Rev. A* **105** 042435
[8] Wu K, Cheng G and Chen A 2020 Tunable asymmetric einstein–podolsky–rosen steering of microwave photons in superconducting circuits *J. Opt. Soc. Am. B* **37** 337–44
[9] Xu X, Chen A, Li Y and Liu Y 2017 Nonreciprocal single-photon frequency converter via multiple semi-infinite coupled-resonator waveguides *Phys. Rev. A* **96** 053853
[10] Xiang Z-L, Ashhab S, You J Q and Nori F 2013 Hybrid quantum circuits: superconducting circuits interacting with other quantum systems *Rev. Mod. Phys.* **85** 623–53
[11] Togan E *et al* 2010 Quantum entanglement between an optical photon and a solid-state spin qubit *Nature* **466** 730–4
[12] Bernien H *et al* 2013 Heralded entanglement between solid-state qubits separated by three metres *Nature* **497** 86–90
[13] Buckley B B, Fuchs G D, Bassett L C and Awschalom D D 2010 Spin-light coherence for single-spin measurement and control in diamond *Science* **330** 1212–5
[14] Childress L, Gurudev Dutt M V, Taylor J M, Zibrov A S, Jelezko F, Wrachtrup J, Hemmer P R and Lukin M D 2006 Coherent dynamics of coupled electron and nuclear spin qubits in diamond *Science* **314** 281–5
[15] Kolkowitz S, Bleszynski Jayich A C, Unterreithmeier Q P, Bennett S D, Rabl P, Harris J G E and Lukin M D 2012 Coherent sensing of a mechanical resonator with a single-spin qubit *Science* **335** 1603–6
[16] Rabl P, Cappellaro P, Dutt M V G, Jiang L, Maze J R and Lukin M D 2009 Strong magnetic coupling between an electronic spin qubit and a mechanical resonator *Phys. Rev. B* **79** 041302
[17] Bennett S D, Yao N Y, Otterbach J, Zoller P, Rabl P and Lukin M D 2013 Phonon-induced spin-spin interactions in diamond nanostructures: application to spin squeezing *Phys. Rev. Lett.* **110** 156402
[18] Ovartchaiyapong P, Lee K W, Myers B A and Jayich A C B 2014 Dynamic strain-mediated coupling of a single diamond spin to a mechanical resonator *Nat. Commun.* **5** 4429
[19] Kepesidis K V, Bennett S D, Portolan S, Lukin M D and Rabl P 2013 Phonon cooling and lasing with nitrogen-vacancy centers in diamond *Phys. Rev. B* **88** 064105
[20] Wilson-Rae I, Zoller P and Imamoglu A 2004 Laser cooling of a nanomechanical resonator mode to its quantum ground state *Phys. Rev. Lett.* **92** 075507
[21] O'Connell A D *et al* 2010 Quantum ground state and single-phonon control of a mechanical resonator *Nature* **464** 697–703
[22] Yang Y, Kladarić I, Drimmer M, von Lüpke U, Lenterman D, Bus J, Marti S, Fadel M and Chu Y 2024 A mechanical qubit *Science* **386** 783–8
[23] Zhou Y, Wang J-W, Cao L-Z, Wang G-H, Shi Z-Y, Lü D-Y, Huang H-B and Hu C-S 2024 Realization of chiral two-mode Lipkin-Meshkov-Glick models via acoustics *Rep. Prog. Phys.* **87** 100502
[24] Zhou Y, Cao L-Z, Wang Q-L, Hu C-S, Zhang Z-C and Xiong W 2023 Phase-dependent strategy to mimic quantum phase transitions *Frontiers Quantum Sci. Technol.* **1** 1078597
[25] Li P-B, Zhou Y, Gao W-B and Nori F 2020 Enhancing spin-phonon and spin-spin interactions using linear resources in a hybrid quantum system *Phys. Rev. Lett.* **125** 153602
[26] Rabl P, Kolkowitz S J, Koppens F H L, Harris J G E, Zoller P and Lukin M D 2010 A quantum spin transducer based on nanoelectromechanical resonator arrays *Nat. Phys.* **6** 602–8
[27] Ma S-li, Li X-ke, Xie J-kun and Li F-li 2019 Two-mode squeezed states of two separated nitrogen-vacancy-center ensembles coupled via dissipative photons of superconducting resonators *Phys. Rev. A* **99** 012325
[28] Bernien H, Childress L, Robledo L, Markham M, Twitchen D and Hanson R 2012 Two-photon quantum interference from separate nitrogen vacancy centers in diamond *Phys. Rev. Lett.* **108** 043604
[29] Sipahigil A, Goldman M L, Togan E, Chu Y, Markham M, Twitchen D J, Zibrov A S, Kubanek A and Lukin M D 2012 Quantum interference of single photons from remote nitrogen-vacancy centers in diamond *Phys. Rev. Lett.* **108** 143601
[30] Li X-X, Li P-B, Ma S-Li and Li F-Li 2017 Preparing entangled states between two NV centers via the damping of nanomechanical resonators *Sci. Rep.* **7** 14116

[31] Einstein A, Podolsky B and Rosen N 1935 Can quantum-mechanical description of physical reality be considered complete? *Phys. Rev.* **47** 777–80
[32] BELL J S 1966 On the problem of hidden variables in quantum mechanics *Rev. Mod. Phys.* **38** 447–52
[33] Schrödinger E 1935 Discussion of probability relations between separated systems *Proc. Cambridge Phil. Soc.* **31** 555–63
[34] Bowles J, Vértesi T, Quintino M T and Brunner N 2014 One-way einstein-podolsky-rosen steering *Phys. Rev. Lett.* **112** 200402
[35] Yang Z, Liu X, Yin X, Ming Y, Liu H and Yang R 2021 Controlling stationary one-way quantum steering in cavity magnonics *Phys. Rev. Appl.* **15** 024042
[36] Liao C, Xie H, Chen R, Ye M and Lin X 2020 Controlling one-way quantum steering in a modulated optomechanical system *Phys. Rev. A* **101** 032120
[37] Kong D, Xu J, Tian Y, Wang F and Hu X 2022 Remote asymmetric einstein-podolsky-rosen steering of magnons via a single pathway of bogoliubov dissipation *Phys. Rev. Res.* **4** 013084
[38] Händchen V, Eberle T, Steinlechner S, Samblowski A, Franz T, Werner R F and Schnabel R 2012 Observation of one-way einstein–podolsky–rosen steering *Nat. Photon.* **6** 596–9
[39] Wollmann S, Walk N, Bennet A J, Wiseman H M and Pryde G J 2016 Observation of genuine one-way einstein-podolsky-rosen steering *Phys. Rev. Lett.* **116** 160403
[40] Xiao Y, Ye X, Sun K, Xu J, Li C and Guo G 2017 Demonstration of multisetting one-way einstein-podolsky-rosen steering in two-qubit systems *Phys. Rev. Lett.* **118** 140404
[41] Tischler N *et al* 2018 Conclusive experimental demonstration of one-way einstein-podolsky-rosen steering *Phys. Rev. Lett.* **121** 100401
[42] He Q, Rosales-Zárate L, Adesso G and Reid M D 2015 Secure continuous variable teleportation and einstein-podolsky-rosen steering *Phys. Rev. Lett.* **115** 180502
[43] Reid M D 2013 Signifying quantum benchmarks for qubit teleportation and secure quantum communication using einstein-podolsky-rosen steering inequalities *Phys. Rev. A* **88** 062338
[44] Chiu C, Lambert N, Liao T, Nori F and Li C 2016 No-cloning of quantum steering *npj Quantum Inf.* **11** 16020
[45] Armstrong S, Wang M, Teh R Y, Gong Q, He Q, Janousek J, Bachor H, Reid M D and Lam P K 2015 Multipartite Einstein-Podolsky-Rosen steering and genuine tripartite entanglement with optical networks *Nat. Phys.* **11** 1745–2481
[46] Xiang Y, Kogias I, Adesso G and He Q 2017 Multipartite gaussian steering: monogamy constraints and quantum cryptography applications *Phys. Rev. A* **95** 010101
[47] Kogias I, Xiang Y, He Q and Adesso G 2017 Unconditional security of entanglement-based continuous-variable quantum secret sharing *Phys. Rev. A* **95** 012315
[48] Gehring T, Händchen V, Duhme J, Furrer F, Franz T, Pacher C, Werner R F and Schnabel R 2015 Implementation of continuous-variable quantum key distribution with composable and one-sided-device-independent security against coherent attacks *Nat. Commun.* **6** 2041–1723
[49] Branciard C, Cavalcanti E G, Walborn S P, Scarani V and Wiseman H M 2012 One-sided device-independent quantum key distribution: security, feasibility and the connection with steering *Phys. Rev. A* **85** 010301
[50] Nathan W *et al* 2016 Experimental demonstration of gaussian protocols for one-sided device-independent quantum key distribution *Optica* **3** 634–42
[51] Li C, Chen K, Chen Y, Zhang Q, Chen Y and Pan J 2015 Genuine high-order einstein-podolsky-rosen steering *Phys. Rev. Lett.* **115** 010402
[52] Scully M O and Zubairy M S 1997 *Quantum Optics* (Cambridge University Press)
[53] Meystre P and Sargent M 2007 *Elements of Quantum Optics* (Springer Science & Business Media)
[54] Guo Y, Li K, Nie W and Li Y 2014 Electromagnetically-induced-transparency-like ground-state cooling in a double-cavity optomechanical system *Phys. Rev. A* **90** 053841
[55] Hu X 2015 Entanglement generation by dissipation in or beyond dark resonances *Phys. Rev. A* **92** 022329
[56] Agarwal G S 1990 Dressed-state lasers and masers *Phys. Rev. A* **42** 686–8
[57] Zakrzewski J, Segal D and Lewenstein M 1992 Pulsed dressed-state lasers *Phys. Rev. A* **46** 2877–86
[58] Scully M O and Zubairy M S 1999 Quantum optics
[59] Uola R, Costa A C S, Nguyen H C and Gühne O 2020 Quantum steering *Rev. Mod. Phys.* **92** 015001
[60] Zhan H, Sun L and Tan H 2022 Chirality-induced one-way quantum steering between two waveguide-mediated ferrimagnetic microspheres *Phys. Rev. B* **106** 104432
[61] Yang Z, Jin H, Jin J, Liu J, Liu H and Yang R 2021 Bistability of squeezing and entanglement in cavity magnonics *Phys. Rev. Res.* **3** 023126
[62] Liu S, Han D, Wang N, Xiang Y, Sun F, Wang M, Qin Z, Gong Q, Su X and He Q 2022 Experimental demonstration of remotely creating wigner negativity via quantum steering *Phys. Rev. Lett.* **128** 200401
[63] Peřina J, Lukš A, Kalaga J K, Leoński W and Miranowicz A 2019 Nonclassical light at exceptional points of a quantum $\mathcal{PT}$-symmetric two-mode system *Phys. Rev. A* **100** 053820
[64] Marangos J P 1998 Electromagnetically induced transparency *J. Mod. Opt.* **45** 471–503
[65] Lukin M D 2003 Colloquium: trapping and manipulating photon states in atomic ensembles *Rev. Mod. Phys.* **75** 457–72
[66] Schmidt H and Imamoglu A 1996 Giant kerr nonlinearities obtained by electromagnetically induced transparency *Opt. Lett.* **21** 1936–8
[67] Kang H and Zhu Y 2003 Observation of large kerr nonlinearity at low light intensities *Phys. Rev. Lett.* **91** 093601
[68] Turek Y, Li Y and Sun C P 2013 Electromagnetically-induced-transparency–like phenomenon with two atomic ensembles in a cavity *Phys. Rev. A* **88** 053827
[69] Hu Y, Liu W, Sun Y, Shi X, Jiang J, Yang Y, Zhu S, Evers J and Chen H 2015 Electromagnetically-induced-transparency–like phenomenon with resonant meta-atoms in a cavity *Phys. Rev. A* **92** 053824
[70] Gardiner C and Zoller P 2004 *Quantum Noise: a Handbook of Markovian and non-Markovian Quantum Stochastic Methods With Applications to Quantum Optics* (Springer Science & Business Media)
[71] Zhou B-yuan, Liu Y, Tan H and Li G-xiang 2021 Chiral-dissipation-assisted generation of entanglement and asymmetric gaussian steering in a driven cascaded quantum network *Phys. Rev. A* **104** 022402
[72] He Q Y, Drummond P D and Reid M D 2011 Entanglement, EPR steering and Bell-nonlocality criteria for multipartite higher-spin systems *Phys. Rev. A* **83** 032120
[73] Reid M D 2013 Monogamy inequalities for the einstein-podolsky-rosen paradox and quantum steering *Phys. Rev. A* **88** 062108
[74] Srensen A and Mlmer K 1999 Spin-spin interaction and spin squeezing in an optical lattice *Phys. Rev. Lett.* **83** 2274–7

[75] Shao X, Ling Y, Yang X and Xiao M 2016 Control of atomic spin squeezing via quantum coherence *Phys. Rev. A* **93** 063825
[76] Ekinci K and Roukes M 2005 Nanoelectromechanical systems *Rev. Sci. Inst.* **76** 061101
[77] Xin J, Lu X-M, Li X and Li G 2020 One-sided device-independent quantum key distribution for two independent parties *Opt. Express* **28** 11439–50
[78] He Q Y and Reid M D 2013 Genuine multipartite einstein-podolsky-rosen steering *Phys. Rev. Lett.* **111** 250403
[79] Opanchuk B, He Q Y, Reid M D and Drummond P D 2012 Dynamical preparation of einstein-podolsky-rosen entanglement in two-well Bose-Einstein condensates *Phys. Rev. A* **86** 023625
[80] Branciard C, Rosset D, Gisin N and Pironio S 2012 Bilocal versus nonbilocal correlations in entanglement-swapping experiments *Phys. Rev. A* **85** 032119
[81] Opanchuk B, Arnaud L and Reid M D 2014 Detecting faked continuous-variable entanglement using one-sided device-independent entanglement witnesses *Phys. Rev. A* **89** 062101
[82] Branciard C, Rosset D, Liang Y-C and Gisin N 2013 Measurement-device-independent entanglement witnesses for all entangled quantum states *Phys. Rev. Lett.* **110** 060405
[83] Gheorghiu A, Wallden P and Kashefi E 2017 Rigidity of quantum steering and one-sided device-independent verifiable quantum computation *New J. Phys.* **19** 023043
[84] He Q Y, Gong Q H and Reid M D 2015 Classifying directional gaussian entanglement, einstein-podolsky-rosen steering and discord *Phys. Rev. Lett.* **114** 060402
[85] Routh E J 1877 *A Treatise on the Stability of a Given State of Motion, Particularly Steady Motion: Being the Essay to Which the Adams Prize was Adjudged in 1877, in the University of Cambridge* (Macmillan and Company)
[86] Hurwitz A 1895 Ueber die bedingungen, unter welchen eine gleichung nur wurzeln mit negativen reellen theilen besitzt *Math. Ann.* **46** 273
[87] DeJesus E X and Kaufman C 1987 Routh-hurwitz criterion in the examination of eigenvalues of a system of nonlinear ordinary differential equations *Phys. Rev. A* **35** 5288–90